Eur. Phys. J. B **50**, 491–496 (2006)
DOI: 10.1140/epjb/e2006-00149-2

THE EUROPEAN PHYSICAL JOURNAL B

Viscoelastic properties of multiwalled carbon nanotube solutions

I. Echeverría[a] and A. Urbina[b]

Department of Chemistry, University of Wisconsin–Madison, 1101 University Avenue, Wisconsin 53706, USA

Received 1st April 2005 / Received in final form 21 December 2005
Published online 5 May 2006 –

Abstract. We have prepared solutions of multiwalled carbon nanotubes in very low vapour pressure solvents (a mixture of chlorinated biphenyls). The solutions are stable and show no sign of precipitation for six months. Rheological measurements using a modified Birnboim apparatus with annular and Sogel-Pochetino geometries have been performed. Using time-temperature superposition we obtained the real and imaginary part of the complex viscosity coefficient in a frequency range covering eight orders of magnitude and a temperature range from 5 to 50 °C. The data shows unexpected changes in the solution with temperature: for T below 30 °C there appears to be some reorganization or clustering. This self-organization could result in a useful technique to improve the electronic properties of polymer/carbon nanotubes composites used in organic electronic devices.

PACS. 81.07.De Nanotubes – 83.85.Cg Rheological measurements-rheometry – 61.46.-w Nanoscale materials

1 Introduction

Carbon–based fibers have been one of the most thrilling materials developed in recent decades. Their stiffness, combined with their low weight, make them the ideal substitute for metals in the development of structural materials for a wide range of applications, from the aerospace industry to building structures. Ten years ago, the discovery by Sumio Iijima [1] of the "helical microtubules of graphitic carbon", now widely known as carbon nanotubes, was an enormous breakthrough in the development of carbon materials.

Carbon nanotubes hold great promise as an ideal low weight carbon fiber with high strength combined with good flexibility and resilience. The sp^2 hybridization of the carbon atoms in the nanotubes provide three strong in-plane σ bonds. The fourth p_z orbital contains a shared electron allowing for electrical conductance of nanotubes. Compared with the graphene sheet, the total energy of the nanotube is increased by the strain energy associated with the curvature of the nanotube, which increases with decreasing diameter. The σ covalent bonds give great strength to the structure of the nanotube. Single-wall nanotubes have no interlayer interactions. Multi-wall nanotubes have many interesting additional properties arising from the interaction between different layers. The lattice structure of the inner and outer layers are generally incommensurate, however in some cases the interlayer stacking can become correlated, so the shear stress between the nanotube shells can differ widely. Both *ab initio* and empirical potential-based methods [2–4] have been used to calculate the strain energy as a function of the diameter and chirality of nanotubes. They find small deviations from the expected $1/R^2$ behavior. The calculated Young modulus is about 1.2 to 1.8TPa and the shear modulus is about 0.4 to 0.5TPa. Molecular dynamic simulations of the response to mechanical deformation such as bending, twisting and compression, show the instabilities that could appear beyond the linear response, and the mechanism of strain release in the elastic or plastic regime through the formation and translation of defects in the original hexagonal lattice [5].

Those theoretical predictions have been confirmed by nice experiments performed on individual nanotubes. There are different techniques of testing the mechanical properties of nanotubes, some of them based in atomic force microscopy (AFM) in which the tip is used as a local probe for manipulation of the nanotubes. The first approach is based on the deposition of nanotubes on special substrates with nanopores [6] or trenches [7]. If one nanotube adheres to both sides of the "hole" and remains suspended like a bridge, then a controlled load can be applied with the tip of the AFM. The relation between the

[a] *Present address*: DuPont Surfaces, PO Box 88, Buffalo NY 14207, USA.
[b] *Present address*: Dep. de Electrónica, Tecnología de Computadoras y Proyectos, Universidad Politécnica de Cartagena, C/Doctor Fleming s/n, 30202 Cartagena, Spain;
e-mail: aurbina@upct.es

applied force and the obtained strain allows calculation of the Young's and shear moduli of the nanotube, because the deflection of the nanotube involves both bending and shear deformations. The mechanical deformation is highly reversible, the nanotube recovers its initial shape once the tip is retracted. The second approach attaches a single nanotube to the tip of the AFM and extracts it from a mat of entangled nanotubes [8]. Then a tensile-load experiment can be performed by measuring the strain in the axial direction, which can be extremely large (about 5%) before the nanotube breaks, giving also a direct measurement of the breaking strength. Both kinds of experiments have been performed on individual single-wall and multi-wall carbon nanotubes and on ropes of single-wall nanotubes. The obtained values for the measured parameters are in good agreement with theoretical predictions. More recently, viscolelastic measurements of an aqueous suspension of surfactant stabilized single wall carbon nanotubes have been presented. The experimental observation suggests that suspension elasticity originates from bonds between the nanotubes rather than from bending or stretching of individual SWNTs [9]. Furthermore, one of the recent results in self-assembling of carbon nanotubes is experimental evidence of a lyotropic liquid crystalline phase of MWNT in aqueous dispersion reported by Song et al [10]. This phase had been theoretically proposed using a continuum-based density-functional theory [11].

One of the applications of the excellent mechanical properties of CNTs is to reinforce a polymeric matrix using them as fillers in composites. For them to be effective the load should be effectively transferred between the matrix and the nanotubes, then the modulus of the composite should be similar to that of randomly oriented CNTs acting like "fibers" of extremely high modulus and strength. Some experiments have been performed to study multi-wall CNT-epoxy composites [12] and thin polymeric films of urethane/diacrylate oligomer dispersed onto graphite powder which contains some amount of carbon nanotubes [13]. In both cases promising results of high load transfer efficiency have been obtained, at least one order of magnitude larger than in conventional fiber-based composites. Also composites of CNTs and conducting polymers (PPV) have been characterized, in this case looking for a significant improvement of the electronic properties of the conducting polymer. An increase in the conductivity by a factor of 10^8 has been reported [14] demonstrating that the dominant conductor is the nanotube, which also acts as a nanometric heat sink preventing the degradation of the polymeric device.

In order to characterize the mechanical behaviour of this kind of composite material it is necessary to use instruments which can measure the properties of the bulk material with nanometric precision in displacements. AFM or local probe individual nanotube measurements cannot be extrapolated to the bulk. We have used rheological measurement techniques to characterize the viscoelastic properties of multiwalled carbon nanotube solutions, and our first results suggest that this is a useful method that could be used to characterize different kinds of carbon nanotube-polymer solutions.

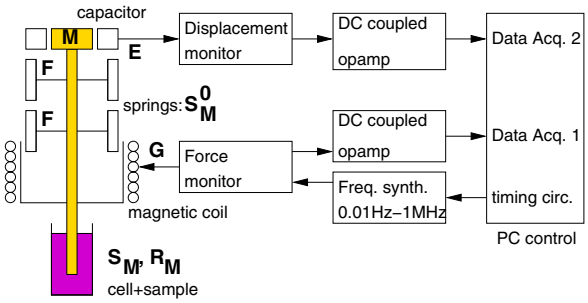

Fig. 1. Simplified schematic of the modified Birnboim apparatus used in the viscoelastic measurements. The force is applied using a magnetic coil and the displacement is measured using a capacitance effect which allows to detect nanometric displacements. The data acquisition system performs cross-correlation statistics over a high number of points to improve the signal/noise ratio. All the system is held at constant temperature using a high precision temperature controller (not shown in the figure).

2 Experimental technique

We have used the "modified Birnboim apparatus", developed at the University of Wisconsin, Madison, by D.J. Massa and J.L. Schrag, which is sufficiently sensitive and precise to measure infinite-dilution properties over a wide frequency range [15,16].

In Figure 1 we show a simplified schematic of this instrument. The instrument applies a force to the sample and measures the strain produced. The force is applied using a magnetic coil transducer which produces very small displacements which are detected using a capacitance sensor with nanometric resolution. The viscoelastic properties of the sample can be calculated by solving the equation of motion for an equivalent mechanical model of the system. A more detailed description of the technique can be found in reference [16]. The motion of part of the apparatus (colored in Fig. 1) must be specifically taken into account in the equations of the equivalent mechanical model. The movable parts are attached to the fixed parts by custom made springs. We can define a Z_M^* "mechanical impedance", as the complex ratio of force to velocity of the moving elements. We introduce the constants, M, mass of the moving elements and S_M^0, spring constants which are the force per unit displacement in the axial direction of the springs. The sample is placed in a cylindrical cell, and its effect is introduced via two parameters: S_M, the "elastance" of the sample (force per unit displacement in phase with displacement) and R_M, the "frictance" of the sample (force per unit velocity in phase with velocity). From these definitions it is easy to write the equations for the shear stress relaxation modulus, $G^* = G_m e^{i\delta} = G' + iG''$, the two components meaning the in-phase and $\pi/2$-out of phase components in complex notation. We begin writing the equation of motion for the moving element driven by

a sinusoidal applied force:

$$Z_M^* = f^*/v = R_M + iX_M = R_M + i(\omega M - S_M/\omega - S_M^0/\omega), \quad (1)$$

by analogy with AC circuit analysis, we could talk about a mechanical resistance R_M and a mechanical reactance X_M, where f^* is a complex force with a real component in phase with velocity and an imaginary component $\pi/2$-out of phase. Our basic measurements are the ratio of the peak values of force and displacement (f_0/x_0) and the phase angle between f_0 and x_0. Using these quantities, we can write:

$$Z_M^* = (f_0/v_0)(\sin\theta - i\cos\theta) = \frac{f_0}{\omega X_0}(\sin\theta - i\cos\theta) \quad (2)$$

$$G' = S_M/b = (-\omega X_M + \omega^2 M - S_M^0)/b \quad (3)$$

$$G'' = \omega R_M/b. \quad (4)$$

The parameter b depends on the kind of cell used in the measuremens:

$$b = \frac{2\pi L}{\ln q - (q^2-1)/(q^2+1)} \quad (5)$$

$$b = \frac{2\pi L}{\ln q}, \quad (6)$$

where $q = R_2/R_1$ is the ratio between the outer and inner radii of the cylindrical cells used in the experiments, L is the length of the inner cylinder introduced in the outer cylinder. The sample is located between both cylinders. Equation (5) applies for the usual "annular"geometry and equation (6) for the "Sogel-Pochetino" geometry in which bottom-free cylinders are used when high viscosity samples have to be measured.

Data are usually reported in terms of the frequency dependent complex viscosity:

$$\eta^* = G^*/(i\omega) = \eta' - i\eta'', \quad (7)$$

where $\eta' = G''/\omega$ is the dynamic viscosity or storage term and $\eta'' = G'/\omega$ is the $\pi/2$-out of phase viscosity or loss term. Finally, the corrected equations including effects of sample inertia, which we used in our measurements are:

$$\eta' = \frac{1}{A}\left(\kappa\frac{f_0}{X_0 R}\frac{\sin\theta}{\omega} - R_M^0\right) \quad (8)$$

$$\eta'' = \frac{1}{\omega A}\left(\kappa\frac{f_0}{X_0 R}\cos\theta - S_M^0 + \omega^2(m + \beta A\rho)\right), \quad (9)$$

where A and β, called the "cell constants", are carefully calibrated for every cell using pure viscous fluids; S_M^0 and R_M^0 are instrument constants that can be obtained from runs with no sample present; and κ is a parameter that has to be calculated for every run of the apparatus using the low frequency response, where $S_M^0 \ll S_M$.

Working frequencies extend from 10^{-2} to 1000 Hz, and time-temperature superposition may extend the effective frequency range to as many as 14 decades [15], typically providing information about macromolecule dynamics that ranges from the slowest overall motions of a chain to rearrangements involving motional distances of a few repeat units, and at the same time providing essential temperature dependence information.

Viscoelastic measurements of solutions, extrapolated to infinite dilution, of relatively stiff and long macromolecules provide a way to characterize some of their physical properties, like Young's modulus, shear modulus, length and (some) length distribution information. This is possible because for fairly rigid macromolecules these properties are governed by the overall rotation and flexural modes of motion induced by the driving shear field. The data typically enable determination of the rotational relaxation time τ_0 (from which length and length distribution information are obtained); and also the relaxation time τ_{1F} for the slowest flexural mode - together with flexural mode relaxation time distribution information - from which Young's modulus (or the shear modulus) is obtained; and sometimes the uniformity of stiffness along the major axis of the molecule can be assessed as well. However, in order to obtain such characterization information it is essential to make measurements at several concentrations in the vicinity of and below the overlap concentration to enable extrapolation to infinite dilution, and the inverse of the relaxation times τ_i involved must be such that the ω_i for which $\omega_i\tau_i$ for all i, lie well within the working frequency range of the instruments.

If a series of measurements are performed at different and low enough concentrations, it is also possible to obtain isolated molecule properties by extrapolation to infinite dilution. In these experiments, the measured response of a solution is taken to be the sum of the macromolecule and solvating environment contributions and can be expressed in terms of shear viscosity or shear modulus. The experimental data can be analyzed using simple mechanical models of macromolecules to obtain information on the conformational dynamics of the macromolecules, as well as macromolecule–solvent and macromolecule–macromolecule interactions [15].

For the case of CNTs, in order to obtain a diameter resolution of 0.1 nm it is necessary to measure the ratio τ_0/τ_{1F} of the relaxation time for end-to-end rotation (τ_0) to that for the first flexural mode (τ_{1F}) with as high precision as possible. Since even one time/temperature superposition step introduces approximately 10 percent uncertainty in this ratio, time/temperature superposition should ideally be avoided. Nevertheless, here we report the first viscoelastic measurements for multiwalled carbon nanotube solutions, proving that this well tested rheological technique can be useful to characterize carbon nanotube solutions and carbon nanotube/polymer composites.

3 Viscoelastic measurements

We have prepared stable solutions of multiwalled carbon nanotubes in poly-chlorinated biphenyls, very low vapour pressure solvents commercially known by the trade name "Aroclor". The solutions have been stable for months and show no signs of incipient precipitation. We used purified

arc-discharge soot material containing multiwalled carbon nanotubes (MWNTs). Aroclors have a strong temperature dependent viscosity, so they are ideal solvents for our viscoelastic measurements. It should be emphasized that carbon nanotubes have been difficult to handle in solution; only using appropriate surfactants it is possible to prepare aqueous suspensions. Recent advances in carbon nanotube functionalization have made it possible to prepare stable solutions in solvents such as toluene or 1,2-dichlorobenzene [17,18]. We attribute our succes in preparing these solutions of MWNTs without functionalization to the biphenyl structure present in the Aroclor which enhances nanotube wrapping by the solvent molecule.

The main drawback of Aroclors is that they are hazardous and one of the most highly regulated chemical compounds in existence. The stock at the University of Wisconsin have been used to prepare our samples, and special security measures have been taken (including use of respirators), more details about the safety cards of Aroclors can be found at the Agency for Toxic Substances and Disease Registry (`http://www.atsdr.cdc.gov`). The disposal of Aroclor contaminated materials was done by the University of Wisconsin according to existing regulations.

Aroclor viscosity can be chosen at will over the range from 0.08 to 6,000 poise. This property is used to our advantage since when we dissolve macromolecules in a viscous solvent, the solvent slows down the dynamics of the macromolecule, bringing it to within the experimental frequency window of our instrument.

In our case, we have chosen Aroclor 1254 (54% chlorine, with 327 average molecular mass). The solution preparation technique involves acid treatment to purify the nanotubes, subsequent filtering and diluting in 1,2 dichloroethane in an ultrasonic bath to untangle the ropes. The dichloroethane is then evaporated, after which the MWNT sample is mixed with the desired Aroclor solvent, then heated and sonicated again, which eventually results in the solutions noted above. (Details of sample preparation along with transport measurements have been given in reference [19]).

Viscoelastic measurements carried out to check MWNT solution stability were made on 0.005 g/cm^3 MWNT/A1254 solutions. Note that this concentration is the total concentration of the MWNT sample in solution.

We present in Figure 2 measurements of the viscoelastic properties of one such solution with a concentration of nanotubes $c = 0.005$ g/cm^3, in a range of temperatures from 4.9 to 46.8 °C. As mentioned before, to obtain the viscoelastic properties of the solution our instrument applies a sinusoidal force of variable frequency, which produces a simple shearing flow of small amplitude in the solution, and measures the response of the sample at the same frequency. Our temperature range could allow us, in principle, to analyze a wide effective frequency range (more than eight decades) if time-temperature superposition can be used.

Figure 3 shows a reduced plot for imaginary (loss, η'') part of the complex shear viscosity, at a reference temperature of 25.5 °C. We have obtained this reduced master curve using time-temperature superposition, which assumes that there is only one mechanism present in the response or that all mechanisms have the same temperature dependence. The branching of the curve in the effective frequency range of 10 to 100 Hz indicates failure of time-temperature superposition also found when analizing η' and reflects changes in the solution with temperature, not scatter in the data. Since these changes are temperature reversible, we rule out any chemical degradation in the sample. In Figure 4 we plot the scale factor, $\log(a_T)$, which shows a marked difference in behaviour between measurements taken below and above 30 °C. Data taken at temperatures above 30 °C can be superposed. However, for $T \leq 30$ °C there appears to be additional mechanisms at play, possibly substantial reorganization or clustering. The shoulder around $\omega a_T = 10^2$, suggests incipient formation

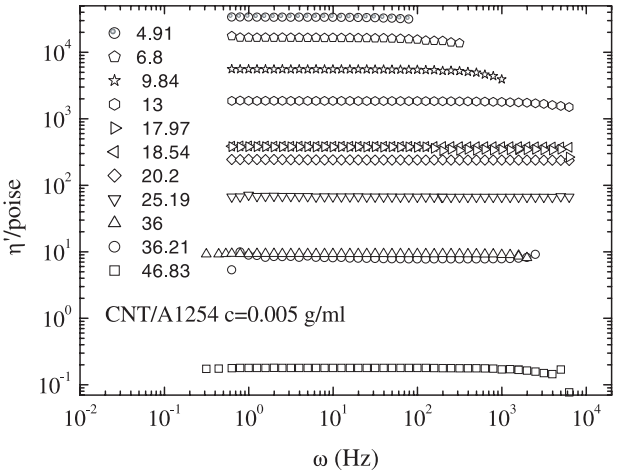

Fig. 2. Log–log plot of the real part of the complex viscosity η' versus frequency for several temperature units indicated in the legend.

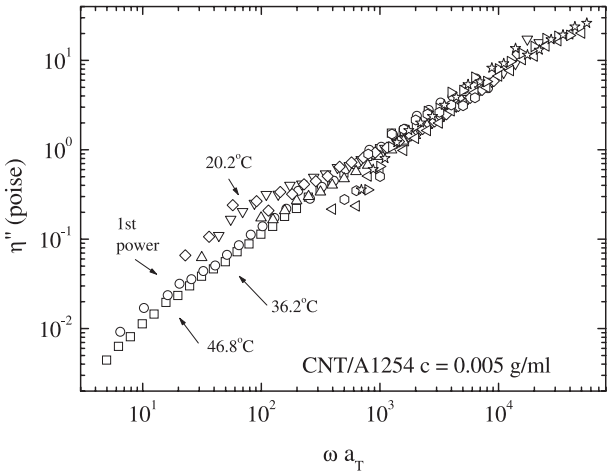

Fig. 3. Log–log plot of the imaginary part of the complex shear viscosity versus reduced frequency. Experimental data for several temperatures have been time/temperature superposed (using a superposition parameter a_T) at a reference temperature $T_0 = 25.2$ °C.

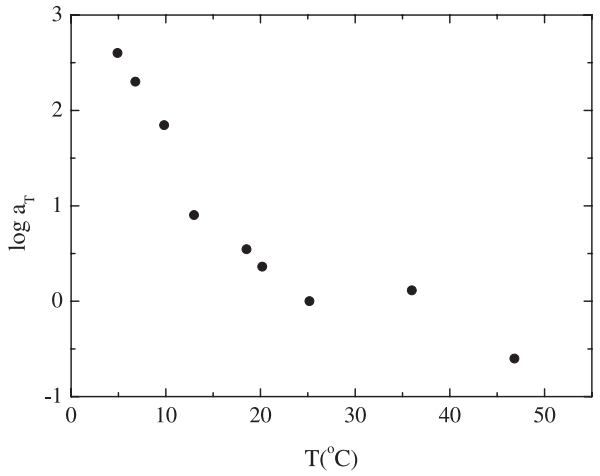

Fig. 4. The scale factor, $\log(a_T)$, used to obtain the master curve of Figure 3, plotted against temperature. The behaviour below and above 30 °C is clearly different.

of a new phase. We explain this transition taking into account that our sample has a mass fraction MWNT/solvent well above the overlapping concentration C^* of the nanotubes. The presence of overlapping in our samples should provide a percolation path between the nanotubes in solution. This is consistent with our estimations of the critical density, d_c, for different solutions of carbon nanotubes with length $l = 1.5$ μm, if they were single walled (10,10) nanotubes, $d_c = 1.43 \times 10^{-6}$ g/cm^3, if they were multiwalled with ten layers, then $d_c = 1.12 \times 10^{-5}$ g/cm^3. These percolation paths can be used as electronic transport channels acting as electron acceptors in the solutions. If we use conjugated polymers as the matrix for carbon nanotube/polymer composites, we get a realization of the "bulk heterojunction" concept with two interpenetrating networks, one acting as electron donor (the conjugated polymer) and the other as electron acceptor (the percolation nanotube network). A complementary demonstration using electronic transport measurements of the existence of a MWNT percolative path in our samples can be found in reference [19].

Thus, we can consider our solutions as an associated rigid rod network. The predicted van der Waals interaction in such systems is very strong, $E_{bond} = 40k_BT$/nm for single wall carbon nanotubes [20]. Viscoelastic measurements of surfactant–covered SWNTs have given experimental results in good agreement with this theoretical prediction [9]. We think that our MWNTs, not covered by any surfactant, should also have a strong interaction due to van der Waals forces. The shape of the curves in Figure 3 suggests that the elasticity of our percolation network is best explained by a punctual bonding of the nanotubes, rather than bending or stretching of the nanotube, following the "percolation on elastic networks with bond-bending forces" model explained in reference [21]. For temperatures above 30 °C the bond breaks and the strain induces a fluidification: the nanotubes disentangle from the pinned percolation network, but no clear evidence of the formation of a liquid crystalline phase was found in our samples.

4 Conclusion

We have used well tested rheological techniques to measure the mechanical properties of multiwalled carbon nanotube solutions. We have obtained the usual viscoelastic parameters (η^*, G^*) for such solutions. This is a different approach to the study of carbon nanotube mechanical properties, in which collective measurements are performed, in contrast with individual AFM or local-probe techniques. Temperature dependent reorganization or clustering suggests incipient formation of a new phase, that could be explained by punctual bonding of the nanotubes in the percolation network, which is formed when the density of nanotubes is well above the critical density. This clustering should be taken into account in order to understand the self-organization mechanisms of the nanotubes in solution. This could give rise to controlled nanostructuration of the composites of conjugated polymers and carbon nanotubes. Improved electronic transport properties could result from this reorganization.

New measurements at different and sufficiently low concentrations should be performed in order to obtain isolated molecule properties by extrapolation to infinite dilution allowing exploration of the concentration and temperature dependence of the observed phase change. Since Aroclors have very restrictive regulations and have to go through an approval process to even have these chemicals present in the laboratory, and considering that we have moved to different labs, we hope to continue this research work using functionalized carbon nanotubes [17], [18] that can be disolved in toluene at concentrations well above the overlapping critical concentration.

We gratefully acknowledge Professor John Schrag for helpful scientific discussions, for allowing use of his equipment and for supplying Aroclor solvents. This work has been partially supported by MCyT (Spain) under Grant MAT2003-04887 and by Fundación Séneca (Murcia, Spain) under Grant PC-MC/1/00064/FS/02.

References

1. S. Iijima, Nature **354**, 56 (1991)
2. J.P. Lu, Phys. Rev. Lett. **79**, 1297 (1997)
3. E. Hernández, C. Goze, P. Bernier, A. Rubio, Phys. Rev. Lett. **80**, 4502 (1998)
4. J. Bernholc, C. Brabec, M.B. Nardelli, A. Maiti, C. Roland, B.I. Yakobson, Appl. Phys. A **67**, 39 (1998)
5. B.I. Yakobson, C.J. Brabec, J. Bernholc, Phys. Rev. Lett. **76**, 2511 (1996)
6. J.P. Salvetat, J.M. Bonard, N.H. Thomson, A.J. Kulik, L. Forró, W.Benoit, L. Zuppiroli, Appl. Phys. A **69**, 255 (1999)
7. T.W. Tombler, C. Zhou, L. Alexseyev, J. Kong, H. Dai, L. Liu, C.S. Jayanthi, M. Tang, S.Y. Wu, Nature **405**, 769 (2000)

8. M.F. Yu, B.S. Files, S. Arepalli, R.S. Ruoff, Phys. Rev. Lett. **84**, 5552 (2000)
9. L.A. Hough, M.F. Islam, P.A. Janmey, A.G. Yodh, Phys. Rev. Lett. **93**, 168102 (2004)
10. W. Song, I.A. Kinloch, A.H. Windle, Science **302**, 1363 (2003)
11. A.M. Somoza, C. Sagui, C. Roland, Phys. Rev. B **63**, 81043 (2001)
12. L.S. Schadler, S.C. Giannaris, P.M. Ajayan, Appl. Phys. Lett. **73**, 3842 (1998)
13. H.D. Wagner, O. Lourie, Y. Feldman, R. Tenne, Appl. Phys. Lett. **72**, 188 (1988)
14. S.A. Curran, P.M. Ajayan, W.J. Blau, D.L. Carrol, J.N. Coleman, A.B. Dalton, A.P. Davey, A. Drury, B. McCarthy, S. Maier, A. Strevens, Adv. Mat. **10**, 1091 (1998)
15. J.D. Ferry, *Viscoelastic properties of Polymers* (John Wiley & Sons Inc., 1980)
16. T.M. Stokich, D.R. Radtke, C.C. White, J.L. Schrag, J. Rheology **38**, 1195 (1994)
17. M. Alvaro, P. Atienzar, P. de la Cruz, J.L. Delgado, H. Garcia, F. Langa, Chem. Phys. Lett. **386**, 342 (2004)
18. J.L. Delgado, P. de la Cruz, F. Langa, A. Urbina, J. Casado, J.T. Lopez-Navarrete, Chem. Comm. **2004**, 1734 (2004)
19. A. Urbina, I. Echeverría, A. Pérez-Garrido, A. Díaz-Sánchez, J. Abellán, Phys. Rev. Lett. **90**, 106603 (2003)
20. L.A. Girifalco, M. Hodak, R.S. Lee, Phys. Rev. B **62**, 13104 (2000)
21. M. Sahimi, S. Arbabi, Phys. Rev. B **47**, 703 (1993)